

**TABLE 1 Summarized Performances of This Mixer and Its Comparison With Previously Published Data**

	This Work		Ref. 5	Ref. 9	Ref. 8	Ref. 6	Ref. 7
Technology	BiCMOS 0.18 $\mu\text{m}$		BiCMOS 0.25 $\mu\text{m}$	CMOS 130 nm	CMOS 130 nm	CMOS 0.25 $\mu\text{m}$	CMOS 0.18 $\mu\text{m}$
Topology	Double- balanced	Single- ended	Double- balanced	Double- balanced	Double- balanced	Double- balanced	Double- balanced
Matching circuit	No	No	RF and LO	No	No	RF and LO	RF and IF
On-chip balun	Yes	Yes	No	No	No	No	No
RF frequency (GHz)	1.8–2.8	1–12	1.8	2–3	5–6	2–9	1–11
CL (dB)	7.5 <sup>a</sup>	10.1–12.9	5.8 <sup>b</sup>	5.6 <sup>b</sup>	6 <sup>b</sup>	6.4 <sup>b</sup>	6.5 <sup>b</sup>
IP1dB (dBm)	6.2 <sup>a</sup>	8.6–14.4	10	0 at 2.5 GHz	–	4–6.5	4–6 <sup>c</sup>
IIP3 (dBm)	15.4 <sup>a</sup>	16–22.2	19.5	10 at 2.5 GHz	10–14	11.4–14.3	9–13 <sup>c</sup>
LO–RF (dB)	–51.9 <sup>a</sup>	–19 to –51.9	–	–48	<–45	–51	–36
LO–IF (dB)	–47.7 <sup>a</sup>	–63.6 to –26.2	–43	–52	<–45	–36	–
RF RL (dB)	14.5 <sup>a</sup>	9–18.4	–	–	>15	8.6–18	4–32
Gate bias (V)	0	0	0	0.33	0.3	0.45	–
Power consumption (dBm)	0	0	0	0	0	0	3

–, not specified.

<sup>a</sup> Data was measured at 2.4 GHz.

<sup>b</sup> Lowest CL versus RF frequency.

<sup>c</sup> IP1dB and IIP3 were measured between 1 and 12 GHz.

with other published CMOS resistive mixers in Table 1. State of the art performance can be seen from the entirety of features.

#### 4. CONCLUSION

A 0.18- $\mu\text{m}$  CMOS passive mixer with baluns fully integrated in IBM7HP process is reported. The unique features of this mixer include extremely low DC offset due to high LO to RF isolation, and broad-band performance of single IF output, despite the balun narrow-band magnitude balance. If single IF output is used, the mixer exhibits CL of 10.1–12.9 dB at the frequencies of 1–12 GHz, IP1dB of 8.6–14.4 dBm, and IIP3 of 16–22.2 dBm. With differential IF outputs combined, at the operating RF frequency of 2.4 GHz and with the LO power of 10 dBm, the CL is 7.5 dB, the IP1dB is 6.2 dBm, and IIP3 is 15.5 dBm. The LO–RF isolation of –51.9 dB, and the LO–IF isolation of –47.7 dB is achieved at 2.4 GHz. Due to its excellent RF–LO isolation between 2 and 2.4 GHz, both IF ports exhibit DC offset of less than 3 mV with the lowest DC offset of 0.7 mV at 2.4 GHz. This is the lowest DC offset for harmonic mixer without DC cancellation, and the widest bandwidth reported to date. This compact integrated design is suitable for heterodyne and homodyne wireless applications.

#### ACKNOWLEDGMENTS

The authors acknowledge Professor Victor M. Lubecke in EE Department, University of Hawaii at Manoa and Dr. Byung Kwon Park at Hundai Mobis, for valuable discussions and TAPO for facilitating chip fabrication.

#### REFERENCES

1. W. Redman-White and D.M.W. Leenaerts, 1/f noise in passive CMOS mixers for low and zero IF integrated receivers, In: Proc. IEEE ESSCIRC 2001, September, 2001, pp. 41–44.
2. S.A. Mass, Microwave mixers, 2nd ed., Artech House, Boston/London, 1993, pp. 338–339.
3. S.A. Maas, A GaAs MESFET mixer with very low intermodulation, IEEE Trans Microwave Theory Tech MTT- 35 (1987), 425–429.
4. O. Boric-Lubecke, J. Lin, A. Verma, I. Lo, and V.M. Lubecke, Multi-band 0.25  $\mu\text{m}$  CMOS base station chip-set for indirect and direct conversion receivers, IEEE Trans Circuits Syst 55 (2008), 2106–2115.

5. P. Gould, C. Zelle, and J. Lin, A CMOS resistive ring mixer MMICS for GSM 900 and DCS 1800, base station applications, In: 2000 IEEE MTT-S Int. Microwave Symp. Dig., Boston, MA, June 2000, Vol. 1, pp. 521–524.
6. I. Lo, X. Wang, O. Boric-Lubecke, Y. Hong, and C. Song, Wide-band 0.25 $\mu\text{m}$  CMOS passive mixer, In: RWS 2009, January 2009.
7. T. Chang and J. Lin, 1–11 GHz ultra-wideband resistive ring mixer in 0.18 $\mu\text{m}$  CMOS technology, In: IEEE RFIC Symp., San Francisco, CA, June 2006.
8. R. Circa, D. Pienkowski, and G. Boeck, Integrated 130nm CMOS passive mixer for 5 GHz WLAN applications, In: 2005 SBMO/IEEE MTT-S Int. Conf., July 2005, pp. 103–106.
9. R. Circa, D. Pienkowski, G. Boeck, R. Kakerow, M. Mueller, and R. Wittmann, Resistive mixers for reconfigurable wireless front-ends, In: IEEE RFIC Symp., June 2005, pp. 513–516.
10. Y. Furuta, T. Heima, H. Sato, and T. Shimizu, A low flicker-noise direct conversion mixer in 0.13  $\mu\text{m}$  CMOS with dual-mode DC offset cancellation circuits, In: 2007 Topical Meeting on Silicon Monolithic Integrated Circuits in RF Systems, 2007, pp. 265–268.
11. S. Zhou and M. Chang, A CMOS passive mixer with low flicker noise for low-power direct-conversion receiver, IEEE J Solid Circuits 40 (2005), 1084–1093.
12. C. Song, I. Lo, and O. Boric-Lubecke, 2.4 GHz 0.18  $\mu\text{m}$  CMOS passive mixer with integrated baluns, In: 2009 IEEE MTT-S Int. Microwave Symp. Dig., June 2009, pp. 409–412.
13. B. Razavi, Design of analog CMOS integrated circuits, McGraw-Hill, New York, 2001, pp. 18.

© 2012 Wiley Periodicals, Inc.

## HIGH GAIN INVERTED U SHAPED MINIATURIZED PATCH ANTENNA FOR MULTIBAND WIRELESS APPLICATIONS

**A. Beno and D. S. Emmanuel**

SENSE, VIT University, Vellore Institute of Technology, School of Electronics Engineering, VIT University Vellore, Tamil Nadu 632014, India; Corresponding author: benoaustin@gmail.com

Received 5 May 2012

**ABSTRACT:** A multiband inverted U-shaped antenna with corrugated slits is proposed. The antenna is designed using small rectangular patch antennas connected with a microstrip feed to operate in the frequency





(a)



(b)

**Figure 4** (a) Network analyzer and (b) return loss graph. [Color figure can be viewed in the online issue, which is available at [wileyonlinelibrary.com](http://wileyonlinelibrary.com)]

connecting lengths are adjusted with variations to have matching and proper coupling between the structures. The regular U shape radiating patch is formed with slits on it in an irregular fashion to achieve this complex structure for achieving good antenna characteristics suitable for wireless applications.

The antenna is designed on a finite ground plane with FR4 as dielectric, above which the patch structure is etched. The copper ground dimension is  $5.6 \times 6.7 \text{ cm}^2$  and the FR4 with a dielectric permittivity of  $\epsilon_r = 4.4$  is placed above the ground with height of  $h = 0.24 \text{ cm}$ . The individual rectangular patch structure has a fundamental resonant frequency of 8 GHz as the electrical length of the antenna  $L = 0.2 \text{ cm}$ . The rectangular patch structures are arranged in the form of an inverted U shape. The novel structure with the modified feed makes the antenna to resonate at multiple frequencies shifting from the fundamental resonant frequency. The antenna with multiple bands makes it to cover the wireless bands for commercial applications with high gain.

### 3. RESULTS AND DISCUSSIONS

The antenna structure is simulated using Ansoft HFSS and fabricated for testing. The fabricated antenna and the simulated structures are shown in Figures 2(a) and 2(b).

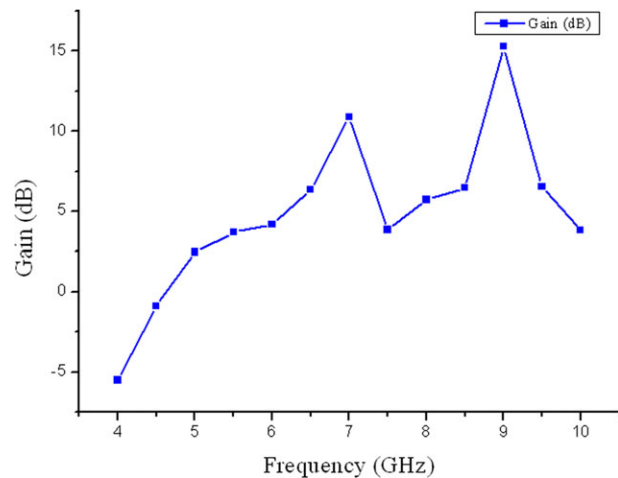


**Figure 5** Gain versus frequency. [Color figure can be viewed in the online issue, which is available at [wileyonlinelibrary.com](http://wileyonlinelibrary.com)]

#### 3.1. Return Loss

The antenna design gives a simulated return loss  $S_{11}$  (dB) of the designed antenna resulted with multiband operating from 5 to 10 GHz with less than  $-10 \text{ dB}$  in all the operating bands. The return loss characteristics shown in Figure 3 exhibit good impedance matching between the feed and the radiating patch. The microstrip feed line is modified with a typical shape and length to meet impedance matching with the radiating patch. The usual design procedures for the feed length and width calculation are adopted and optimized to suit the antenna design.

The simulated antenna design is fabricated and the antenna is tested using Agilent Network analyzer for the return loss characteristics. The prototype fabricated antenna is tested with the network analyzer and its respective return loss characteristics obtained are shown in Figures 4(a) and 4(b). The measured result from network analyzer gives a multiband antenna covering the frequency range from 5 to 10 GHz with good return loss suitable for a radiating antenna structure.

The return loss result shows the antenna operating in multiple bands with less than  $-10 \text{ dB}$  in all the multiple operating bands. The bandwidth of operating bands is determined to show the capability of the antenna meeting the requirements of the

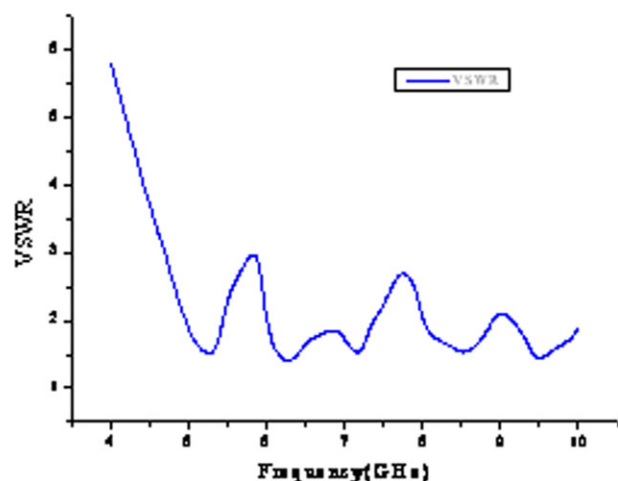


**Figure 6** Frequency versus VSWR of the multiband antenna. [Color figure can be viewed in the online issue, which is available at [wileyonlinelibrary.com](http://wileyonlinelibrary.com)]



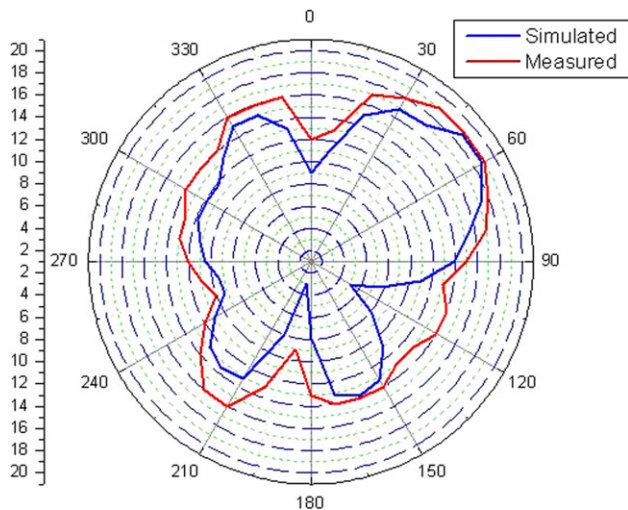


**Figure 7** Radiation pattern for E plane. [Color figure can be viewed in the online issue, which is available at [wileyonlinelibrary.com](http://wileyonlinelibrary.com)]

wireless bands. The operating band of the antenna starts from 5 to 10 GHz covering the WLAN, satellite frequency and Wi-Max applications.

### 3.2. Gain and Directivity

The antenna offers high gain over the entire operating band. The gain of the antenna is above 2 dB in all the multiband frequency. The antenna attains peak gain of 15.29 dB at 9 GHz. The gain for the various operating frequencies in the band from 1 to 10 GHz is plotted and shown in Figure 5.

The antenna has achieved good impedance matching over the entire operating bands. The microstrip feed is designed to have a strip width of  $W_s = 1$  mm and length of the strip is  $L_s = 8.2$  cm. The microstrip feed is coupled with a 50  $\Omega$  SMA connector making the port perfectly matched. The VSWR of the antenna is well below two in all the operating bands as shown in the Figure 6.

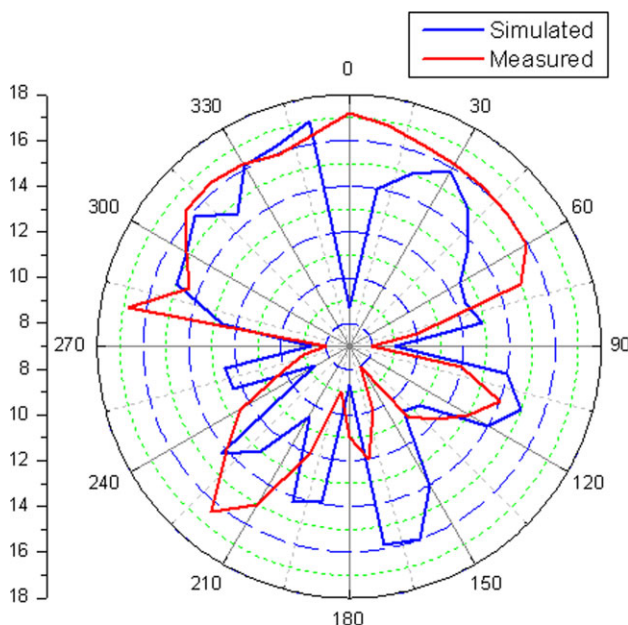


**Figure 8** Radiation Pattern for H plane. [Color figure can be viewed in the online issue, which is available at [wileyonlinelibrary.com](http://wileyonlinelibrary.com)]

### 3.3. Radiation Pattern

The simulated H-Field pattern is shown in Figure 9. The simulated E-field pattern and H-Field pattern at 5 GHz are shown in Figures 7 and 8.

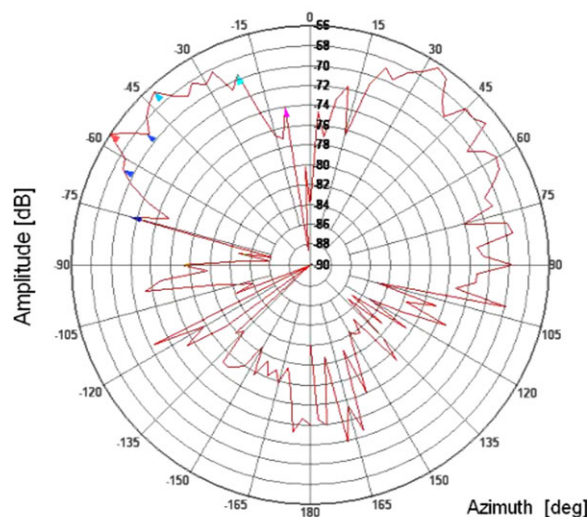
The designed antenna is tested in the anechoic chamber and the radiation pattern for the E- and H-Field is plotted. The antenna exhibits good radiation pattern characteristics providing wide beam angle coverage with high gain of around 8 dB. The simulated radiation pattern with the tested pattern from the anechoic chamber shows the results are in good agreement. The test conducted in the anechoic chamber and the radiation plot from the chamber measurement are given in the Figures 9(a) and 9(b).

## 4. CONCLUSION

The antenna is designed with a novel shape derived from the U-shaped microstrip patch antenna structure. The antenna operated with a multiband frequency making it most suitable for the wireless applications like Wi-Max, WLAN, and Satellite frequency bands in the range from 5 to 10 GHz. The antenna achieves good impedance matching and gain in the entire band of operation. The antenna does serve well in radiating in all frequencies of operation with good radiation efficiency.



(a)



(b)

**Figure 9** (a) Antenna in anechoic chamber and (b) measured radiation pattern. [Color figure can be viewed in the online issue, which is available at [wileyonlinelibrary.com](http://wileyonlinelibrary.com)]

## ACKNOWLEDGMENT

The authors acknowledge the team of TCE Madurai for providing facilities for testing the antenna structure.

## REFERENCES

1. A.H. Reja, Study of microstrip feed line patch antenna, Eng Tech J 27 (2009).
2. M.T. Islam, A.T. Mobashsher, and N. Misran, Design of microstrip patch antenna using novel U-shaped feeding strip with unequal arm, Electron Lett 46 (2010).
3. M. Yang, Y. Chen, R. Mittra, and Z. Gong, U-shaped planar inverted-F microstrip antenna with a U-shaped slot inset for dual-frequency mobile communications, IEEE Proc. Microwave Antennas Propag. 150 (2003), 197–202.
4. J. Ghalibafan and A.R. Attari, A new dual-band microstrip antenna with U-shaped slot, Prog Electromagn Res C 12 (2010), 215–223.
5. M.N. Mahmoud and R. Baktur, A dual band microstrip-fed slot antenna, IEEE Trans Antennas Propag 59 (2011), 1720–1724.
6. K. Seol, J. Jung, and J. Choi, Multi-band monopole antenna with inverted U-shaped parasitic plane, Electron Lett 42 (2006).
7. M. Koohestani and M. Golpour, U-shaped microstrip patch antenna with novel parasitic tuning stubs for ultra wideband applications, Lett Microwave Antennas Propag 4 (2010), 938–946.
8. J.A. Ansari, S.K. Dubey, P. Singh, R.U. Khan, B.R. Vishvakarma, Analysis of U-slot loaded patch for dualband operation, Int J Microwave Opt Technol 3 (2008), 80–84.
9. J.-H. Lu and R.-H. Chen, Planar inverted U-shaped patch antenna with high-gain operation for Wi-Fi/Wimax application, IEEE 2009, pp. 1855–1858.
10. G.A. Mavridis, D.E. Anagnostou, C.G. Christodoulou, and M.T. Chrysomallis, Quality factor Q of a miniaturized meander microstrip patch antenna, IEEE 2008.
11. V.S. Chintakindi, S.S. Pattnaik, O.P. Bajpal, S. Devi, S.V.R.S. Gollapudi, and P.K. Pradyumna, Parameters calculations of rectangular microstrip patch antenna using particle swarm optimization technique, IEEE, 2007.

© 2012 Wiley Periodicals, Inc.

## DUAL-POLARIZED BAND-STOP FSS SPATIAL FILTERS USING VICSEK FRACTAL GEOMETRY

M. R. da Silva,<sup>1</sup> C. de L. Nóbrega,<sup>1</sup> P. H. da F. Silva,<sup>2</sup> and A. G. D'Assunção<sup>1</sup>

<sup>1</sup> Federal University of Rio Grande do Norte, UFRN-CT-DCO, Postal Code 1655, CEP 59078-970, Natal, RN, Brazil; Corresponding author: adaildo@ct.ufrn.br

<sup>2</sup> Federal Institute of Education, Science and Technology of Paraíba, IFPB, CEP 58015-430, João Pessoa, PB, Brazil

Received 5 May 2012

**ABSTRACT:** This article presents a fractal design methodology for frequency selective surfaces (FSSs) by printing a finite planar array of Vicsek fractal metallic patches on a single dielectric layer. Shapes presented by the Vicsek fractal as a function of the fractal parameters (level and scale factor) were exploited to design FSSs acting as dual-polarized band-stop spatial filters for incident plane waves. Transmission properties of these FSSs were analyzed and two FSS prototypes were built and measured to validate the fractal design methodology. The obtained results pointing to interesting FSS properties: a high frequency compression factor of 50.31% and stable resonance frequency at oblique incidence. © 2012 Wiley Periodicals, Inc. Microwave Opt Technol Lett 55:31–34, 2013; View this article online at wileyonlinelibrary.com. DOI 10.1002/mop.27242

**Key words:** frequency selective surfaces; spatial filters; Vicsek fractal

## 1. INTRODUCTION

A band-stop frequency selective surface (FSS) is a two-dimensional array of periodic metallic elements printed on a dielectric layer. When an electromagnetic wave impinges on the surface, each element resonates and scatters energy around its resonant frequency. The incident wave is partly transmitted in the forward direction and partly reflected in the specular direction. These structures resonate at a given frequency, thus exhibiting spectral selectivity [1, 2].

The main parameters that will determine the overall frequency response of a FSS are: the element shape (type and geometry), the substrate parameters, and inter-element spacing (cell-size or periodicity) [2]. FSSs act as spatial filters for plane waves in a variety of applications, such as: radomes, microwave absorbers, dichroic subreflectors, antenna systems, and so forth [1, 2].

Many authors have investigated different types of periodic structures to analyze their properties and performance, such as, reconfigurable FSSs [3], multilayer selective filters [4], periodic arrays printed on anisotropic dielectric substrates [5], and FSSs that use fractal geometry in their design [6–12].

FSS design using fractal elements is becoming a competitive solution that presents many advantages in relation to the conventional FSS design using Euclidian elements. Because of their self-similarity and space-filling fractal properties, geometric fractals can be used to design single layer FSSs with higher frequency compression factor (CF) and the development of compact spatial filters becomes possible. In Refs. 6 and 7, Koch and Dürer geometric fractals were proposed for designing compact FSS filters with CF = 44.27% and CF = 43.52%, respectively. For FSSs designed with Gosper fractal geometry was reported a CF of 23.82% [8].

Other interesting feature of the fractals' application in FSS is ensuring good stability for oblique incidence. Miniaturized angularly stable fractal FSSs were proposed in Refs. 11 and 12. These structures were analyzed according to the variation of different incident angles for both horizontal and vertical polarizations. In Ref. 13 and 14 novel miniaturized periodic elements were used to develop compact FSSs with stable resonance.

In this article, we describe a fractal design methodology for FSSs composed by a periodic structure of Vicsek fractal patches. Shapes presented by the Vicsek fractal as a function of the fractal parameters (level and scale factor) were exploited to design FSSs acting as dual-polarized band-stop spatial filters. We also investigate the oblique incidence of electromagnetic waves according the fractal iteration-number to design compact FSS spatial filters with stable frequency responses.

FSS simulations were performed using Ansoft Designer<sup>TM</sup> and HFSS<sup>TM</sup> softwares considering Vicsek patches up to fractal level  $k = 3$ . The fractal level was limited due to complexity of the resulting fractal patch element geometry. Two FSS prototypes were selected for fabrication and experimental characterization. Measured results were accomplished with the use of a vector network analyzer from Agilent Technologies, model N5230A, and two X-band horn antennas operating in the range of 7.0–13.5 GHz.

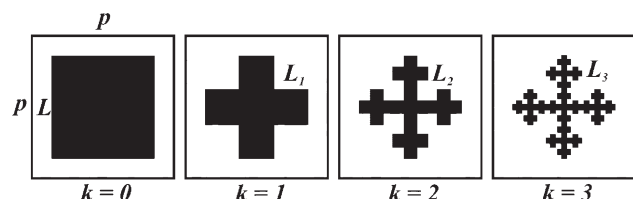


**Figure 1** Vicsek fractal patch elements